Definition and McCARD/DeCART Analysis of Light-Water SMR Core Benchmark Problems Based on NuScale

Seungsu Yuk*, Jin Young Cho
Korea Atomic Energy Research Institute, 111, Daedeok-daero 989beon-gil, Daejeon, 34057, Korea
**Corresponding author: syuk@kaeri.re.kr*

***Keywords :** SMR, NuScale, DeCART, McCARD, Reactor Core Benchmark

1. Introduction

In the pursuit of advanced reactor design, the demand for high-fidelity reactor physics analysis has become increasingly paramount. To enhance the understanding of high-fidelity neutronics and to facilitate the verification and validation (V&V) of advanced core analysis codes, the Korea Atomic Energy Research Institute (KAERI) participated in the US/ROK International Nuclear Energy Research Initiative (I-NERI) project.

One of the tasks in this collaboration was the development of a benchmark suite for light-water Small Modular Reactors (SMRs) based on the NuScale reactor design. Because the detailed specifications for the NuScale reactor were not disclosed, KAERI has developed a new benchmark problem set based on the published documents [1, 2] and the previous works [3, 4].

This paper provides a comprehensive definition of these light-water SMR core benchmark problems to serve as a standard resource for the neutronics community. To establish a reliable baseline, reference solutions were generated using the continuous-energy Monte Carlo code, McCARD [5]. Furthermore, this study presents analysis results from DeCART [6], a whole-core high-fidelity transport code developed by KAERI.

2. Light-Water SMR Core Benchmark Problems

The Light-Water SMR Core Benchmark Problems were constructed based on publicly available specifications of the NuScale reactor. Comprehensive details regarding the geometric configurations and material compositions for each problem are provided in the Appendix.

The benchmark set is structured in a hierarchical manner to facilitate step-by-step verification, encompassing: 1) Single fuel pin problems (2-D), 2) Single fuel assembly problems (2-D), 3) 2-D core problems, 4) 3-D core problems, and 5) a 3D core depletion problem. Except for the 3D core depletion case, which is evaluated under Hot Full Power (HFP) conditions, the benchmark calculations are to be performed across a matrix of parametric variations. These variations are designed to test the code's response to different physical states and are defined as follows:

Moderator/Clad Temperature: 600 K
Fuel Temperature: 600 K and 900 K
Soluble Boron Concentration: 0, 1000, and 2000 ppm

The total number of problems is 49:
1) 12 single fuel pin problems
   (Problem IDs: NS01C01 ~ NS01C12)
2) 24 single fuel assembly problems
   (Problem IDs: NS02A0C01 ~ NS02B2C06)
3) Six 2-D core problems
   (Problem IDs: NS03C01 ~ NS03C06)
4) Six 3-D core problems
   (Problem IDs: NS04C01 ~ NS04C06)
5) One core depletion problem
   (Problem ID: NS05C01)

Detailed descriptions for each specific benchmark problem are further elaborated in the Appendix.

Reference solutions to benchmark problems were produced using the continuous-energy Monte Carlo code McCARD with ENDF/B-VII.1 neutron cross section library. The standard deviation of multiplication factors for McCARD results were within 4~7 pcm.

3. Calculations and Results

The Light-Water SMR Core Benchmark Problems were solved using DeCART, and the results were compared with reference solution obtained by McCARD. The DeCART calculations were conducted with the ENDF/B-VII.1 based 47-group cross section library generated with the KAERI cross section library generation system, which includes resonance integral table, subgroup data [7]. The anisotropic scattering source is treated by the order of P2 developed in [8]. For the ray tracing option, the ray-spacing of 0.02 cm, 4 polar angles of 90, and 8 azimuthal angles of 90 were used.

The calculation results are summarized for each category of benchmark problem as follows.

3.1 Single Fuel Pin Cell Problems

There were 12 single fuel rod problems with 2 kinds of nuclear fuel (U^{235} enrichment: 1.87% and 4.55%) and 6 conditions shown in Section 2. Table I shows the multiplication factor results of McCARD and DeCART calculation and the relative difference between them. The reactivity error is within 100 pcm in the problem. The

DeCART result is well matched with the reference solution (McCARD).

Table I: Multiplication Factor Results for Single Fuel Pin Problems

ID	McCARD	DeCART	Reactivity Difference [pcm]
NS01C01	1.20072	1.20171	69
NS01C02	1.19010	1.19097	61
NS01C03	1.06854	1.06940	75
NS01C04	1.05918	1.05989	63
NS01C05	0.96566	0.96649	89
NS01C06	0.95713	0.95797	92
NS01C07	1.38555	1.38697	74
NS01C08	1.37403	1.37512	58
NS01C09	1.30288	1.30418	77
NS01C10	1.29210	1.29314	62
NS01C11	1.23112	1.23240	84
NS01C12	1.22107	1.22208	68

3.2 Single Fuel Assembly Problems

There were 24 single fuel assembly problems with 4 kinds of assembly (A0, B0, B1, B2, they are described in Appendix) and 6 conditions shown in Section 2. Table II shows the comparison of the multiplication factors between McCARD and DeCART for single fuel assembly benchmark problems. It shows that the average of reactivity difference between two codes is 16 pcm. The largest difference between two results is found at NS02B2C05 problem and the value is 43 pcm.

The comparison of radial pin power distribution between two codes for single fuel assembly benchmark problem is also performed. The average RMS error of radial pin power is calculated to be 0.21%. The average error of radial pin power is found to be 0.10%. The maximum pin power error is 0.49% and it is appeared in NS02B0C01 problem. Fig. 1 shows the radial pin power distribution of NS02B0C01 problem (B0 assembly, Fuel: 600K, Moderator/Clad: 600K, 0 ppm). The other cases are presented in Appendix. The DeCART result is close to the reference solution (McCARD).

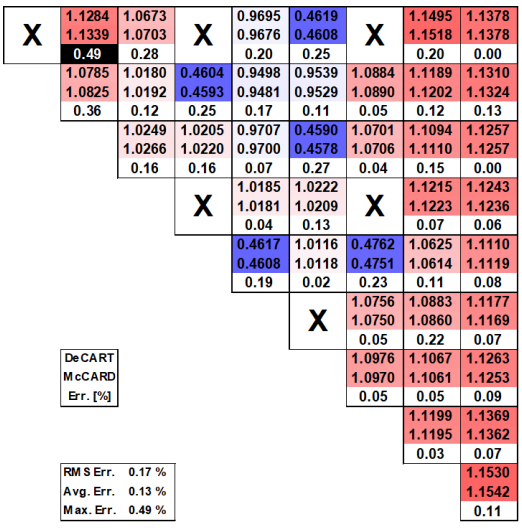

Fig. 1. Pin Power Distribution for 2-D Fuel Assembly Problem: B0 Type, Fuel: 600K, Moderator/Clad: 600K, 0 ppm.

Table II: Multiplication Factor Results for 2-D Fuel Assembly Problems

ID	McCARD	DeCART	Reactivity Difference [pcm]
NS02A0C01	1.41717	1.41750	16
NS02A0C02	1.40620	1.40646	13
NS02A0C03	1.31590	1.31642	30
NS02A0C04	1.30592	1.30625	19
NS02A0C05	1.23041	1.23095	36
NS02A0C06	1.22113	1.22152	26
NS02B0C01	1.13918	1.13924	5
NS02B0C02	1.13088	1.13057	-24
NS02B0C03	1.07545	1.07545	0
NS02B0C04	1.06738	1.06737	-1
NS02B0C05	1.01965	1.01990	24
NS02B0C06	1.01230	1.01232	2
NS02B1C01	1.08320	1.08319	-1
NS02B1C02	1.07499	1.07464	-30
NS02B1C03	1.02428	1.02438	10
NS02B1C04	1.01642	1.01641	-1
NS02B1C05	0.97281	0.97306	26
NS02B1C06	0.96555	0.96558	3
NS02B2C01	1.06830	1.06846	14
NS02B2C02	1.05997	1.05989	-7
NS02B2C03	1.01055	1.01079	23
NS02B2C04	1.00268	1.00279	11
NS02B2C05	0.96003	0.96043	43
NS02B2C06	0.95271	0.95293	24

3.3 2-D Core Problems

There were six 2-D Core Problems with 6 conditions shown in Section 2. Table III shows the comparison of the multiplication factors between McCARD and DeCART for 2-D core benchmark problems. It shows that the average of reactivity difference between two codes is 44 pcm. The largest difference between two results is found at NS03C05 problem and the value is 57 pcm.

The comparison of radial assembly power distribution between two codes is also performed. The average RMS error of radial assembly power is calculated to be 0.43%. The average error of radial assembly power is found to be 0.39%. The maximum assembly power error is 0.74% and it is appeared in NS03C01 problem as shown in Fig. 2. The other cases are presented in Appendix.

Table III: Multiplication Factor Results for 2-D Core Problems

ID	McCARD	DeCART	Reactivity Difference [pcm]
NS03C01	1.10974	1.11033	48
NS03C02	1.10157	1.10183	21
NS03C03	1.04400	1.04446	42
NS03C04	1.03604	1.03654	47
NS03C05	0.98715	0.98771	57
NS03C06	0.97986	0.98031	47

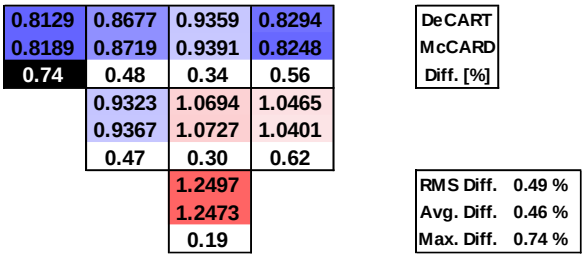

Fig. 2. Radial Assembly Power Distribution for 2-D Core Problem: Fuel: 600K, Moderator/Clad: 600K, 0 ppm.

3.4 3-D Core Problems

There were six 3-D Core Problems with 6 conditions shown in Section 2. Table IV shows the comparison of the multiplication factors between McCARD and DeCART for 3-D core benchmark problems. It shows that the average of reactivity difference between two codes is 9 pcm. The largest difference between two results is found at NS04C02 problem and the value is 18 pcm.

The comparison of radial assembly power distribution between two codes is also performed. The average RMS error of radial assembly power is calculated to be 0.69%. The average error of radial assembly power is found to be 0.64%. The maximum radial assembly power error is 1.16% and it is appeared in NS04C02 problem as shown in Fig. 3. For the axial power comparison, the average RMS error of axial power is calculated to be 0.94%. The average error of axial power is found to be 1.06%. The maximum axial power error is 2.38% and it is appeared in NS04C01 problem as shown in Fig. 4. The other cases are presented in Appendix.

Table IV: Multiplication Factor Results for 3-D Core Problems

ID	McCARD	DeCART	Reactivity Difference [pcm]
NS04C01	1.09846	1.09831	-12
NS04C02	1.09014	1.08993	-18
NS04C03	1.03176	1.03177	1
NS04C04	1.02414	1.02398	-15
NS04C05	0.97519	0.97521	2
NS04C06	0.96801	0.96793	-9

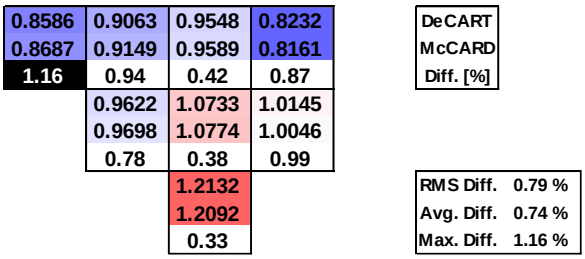

Fig. 3. Radial Assembly Power Distribution for 3-D Core Problem: Fuel: 900K, Moderator/Clad: 600K, 0 ppm.

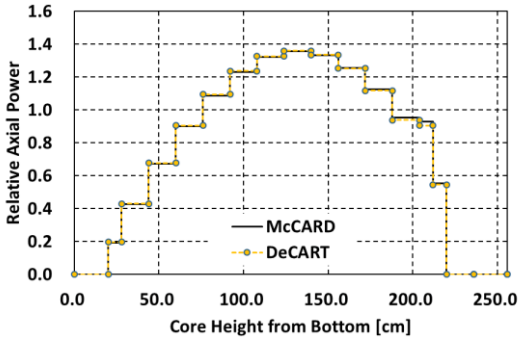

Fig. 4. Axial Power Distribution for 3-D Core Problem: Fuel: 600K, Moderator/Clad: 600K, 0 ppm.

3.5 3-D Core Depletion Problem

This benchmark problem is a problem of calculating the first-cycle depletion at HFP with critical state. The xenon equilibrium state is assumed at each burnup step. The temperature distribution at HFP state should be obtained through thermal fluid analysis. The calculation was performed using DeCART's own thermal fluid analysis module, and the result is shown in Fig. 5. (The reference solution is not provided in this paper.) It shows that the burnable absorber compensates the excess reactivity until 10 MWD/kgHM.

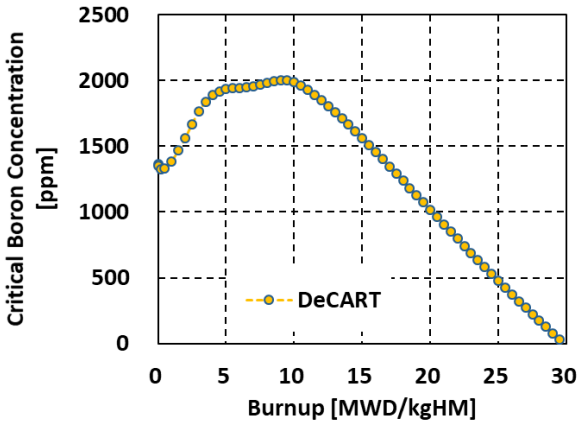

Fig. 5. Critical Boron Concentration for 3-D Core Depletion Problem.

4. Conclusions

In this paper, the light-water SMR reactor core benchmark problems based on the NuScale were described and they were solved by DeCART for the verification and validation. A comparison of the results with the reference code McCARD found that DeCART and McCARD agreed well in most cases. In the 2-D and 3-D core problems, only the effective multiplication factor difference of about several tens of pcm was shown, and there was no significant difference in the power distribution. The first cycle core depletion calculation was performed to verify the multi-physics core analysis function. Taken together, it was confirmed that the DeCART code can carry out advanced small modular reactor core analysis with high accuracy.

In a broader context, benchmark development for SMR cores, such as NuScale-like core benchmark [9], remains a focal point of current research efforts. By providing these detailed specifications and reference solutions as open verification data, this paper aims to support SMR reactor physics groups in their code verification processes. Ultimately, it is expected that this contribution will lead to enhanced analysis accuracy and reliability across the field of SMR core design and safety evaluation.

ACKNOWLEDGEMENTS

This study was supported by the National Research Foundation of Korea (NRF) grant funded by the Korea government (MSIT). (No. 2017M2A8A1092448).

REFERENCES

[1] NuScale Power, LLC., "NuScale Standard Plant Design Certification Application, PART2-TIER2, Chapter 4: Reactor, Revision 5," July 2020.
[2] A. Sadegh-Noedoost, et al., "Investigation of the fresh-core cycle-length and the average fuel depletion analysis of the NuScale core," Annals of Nuclear Energy, vol. 136, pp. 106995, 2020.
[3] Y. H. Choi, et al., "VVER1000 Reactor Benchmark Problems," KAERI/TR-7339/2018, KAERI Technical Report, 2018.
[4] S. Yuk, et al., "APR1400 Reactor Core Benchmark Problems," KAERI/TR-7822/2019, KAERI Technical Report, 2019.
[5] H.J. Shim, et al., "McCARD: Monte Carlo Code for Advanced Reactor Design and Analysis," Nuclear Engineering and Technology, vol. 44, pp.161-176, 2012.
[6] J. Y. Cho and H. G. Joo, "Solution of the C5G7 MOX benchmark three-dimensional extension problems by the DeCART direct whole core calculation code," Progress in Nuclear Energy, vol. 48, pp. 456–466, 2006.
[7] H.J. Park et al., "An improved DeCART library generation procedure with explicit resonance interference using continuous energy Monte Carlo calculation," Annals of Nuclear Energy, vol. 105, pp. 95-105, 2017.
[8] J.Y. Cho et al., "Axial SPN and Radial MOC Coupled Whole Core Transport Calculation," Journal of Nuclear Science and Technology, vol. 44, pp. 1156-1171, 2007.
[9] E. Fridman, et al., "Definition of the neutronics benchmark of the NuScale-like core," Nuclear Engineering and Technology, vol. 55, pp. 3639-3647, 2023.

Appendix A: Benchmark Specification

In this section, the geometry and materials of benchmark problems are described. Most problem specifications are based on the published NuScale design document [1] and journal paper [2].

A.1 General Description of Benchmark Reactor

The benchmark reactor core is composed of 37 fuel assemblies (FA). The FAs are arranged in rectangular lattice in the core. Each FA has 264 fuel or burnable absorber rods. The fuel rods of each FA are arranged in 17 by 17 rectangular lattice. Each FA also has 24 guide tubes (GT) for control rods and 1 central tube (CT) for instruments.

There are four fuel assembly types, A0, B0, B1, and B2 for constructing the reactor core benchmark problem set. For the FA loading pattern in the core and the fuel pin arrangement in the FA, the first cycle of NuScale core in the journal paper [2] is used. The overall dimensions of reactor core are given in Table A.I.

Table A.I: Geometrical Design Data for Benchmark Reactor Core

Parameter	Value
Core	
Total height	256 cm
Top reflector height	20 cm
Bottom reflector height	20 cm
Assembly pitch	21.503 cm
Pin pitch	1.26 cm
Fuel rod, Burnable absorber rod, Top end, Bottom end	
Pellet radius	0.406 cm
Clad inner radius	0.414 cm
Clad outer radius	0.475 cm
Active fuel height	200 cm
Top axial blanket height	8 cm
Bottom axial blanket height	8 cm
Top end height	16 cm
Bottom end height	0 cm
Guide tube and Central tube	
Guide tube inner radius	0.5715 cm
Guide tube outer radius	0.612 cm
Guide tube height	216 cm

A.2 Pin Cell

The geometry of the outer boundary of the pin cell is a square whose pitch is 1.26 cm as shown in Fig.A.1 (a). The radial dimensions of the pin cell and material ID of various pin types are given in Fig.A.2. There are three different types of pin cells; fuel rod, burnable absorber rod, and top end. In the fuel rod, UO2 fuel is loaded in the region #1 (See Fig.A.2. (a)). The region #2 in the fuel rod represents a gap between fuel and cladding. The outside region of the cladding is filled with moderator H2O (MOD). The composition of moderator depends on the soluble boron concentration. The other pin types have the same geometry and material composition except for the region #1 (See Fig.A.2 (b) and (c)).

The guide tube cell and the central tube cell also have square boundary with the same size as shown in Fig.A.1 (b). The radial dimensions and material ID of them are given Fig.A.2 (d). The inside and outside regions of the cladding in Fig.A.2 (d) are also filled with moderator H2O (MOD).

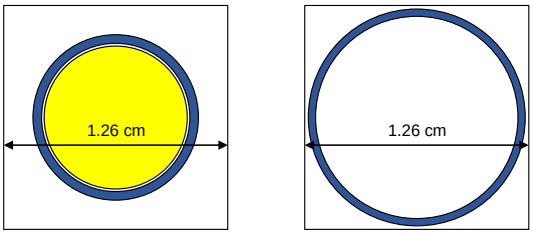

(a) Pin cell (b) Tube cell

Fig. A.1. Square Pin and Tube Cell Size.

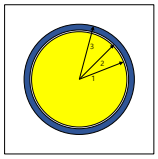

Region #	Size [cm]	Material
1	0.406	UO2 Fuel
2	0.414	AIR
3	0.475	CLD

(a) Fuel rod

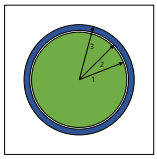

Region #	Size [cm]	Material
1	0.406	GD
2	0.414	AIR
3	0.475	CLD

(b) Burnable absorber rod

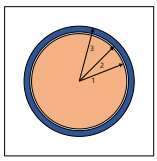

Region #	Size [cm]	Material
1	0.406	MIXSPR
2	0.414	AIR
3	0.475	CLD

(c) Top end

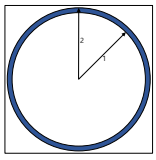

Region #	Size [cm]	Material
1	0.5715	MOD
2	0.612	CLD

(d) Guide tube, Central tube

Fig. A.2. Various Pin Cell and Tube Cell Geometry of Fuel Assembly.

A.3 Fuel Assembly

The outer boundary of the fuel assembly (FA) of Benchmark reactor is a square whose pitch including assembly gap is 21.503 cm as shown in Fig.A.3. The assembly gap is filled with the moderator of H2O (MOD). The details of dimensions of FA are in Table A.II. Each FA is made up of 264 square pin cells (Fig.A.1 (a)) and 25 tube cells (Fig.A.1 (b)).

There are 4 types of fuel assemblies, A0, B0, B1, and B2. These are distinguished by the weight fraction of burnable absorber. The detail of each type is illustrated in Fig.A.4 through Fig.A.7. The uranium enrichment of all fuel pin cells is 4.55 wt%. A0 does not have any burnable absorber pin cells. B0~B2 have 32 burnable absorber rods. The weight fraction of burnable absorber in FA is shown in Table A.III.

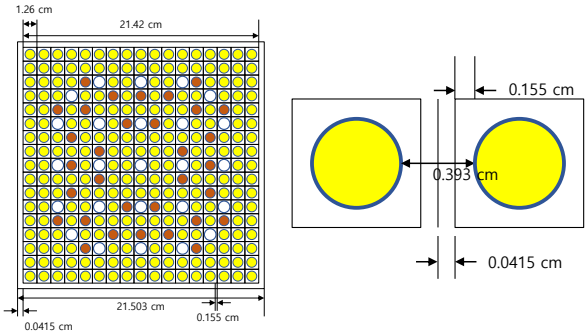

(a) Fuel assembly (b) Assembly gap

Fig. A.3. Geometry of Fuel Assembly.

Table A.II: Dimensions of Fuel Assembly

Parameter	Value
Fuel assembly size	
Number of pin cells in a side of FA	17
Number of pin cells in FA	264
Number of tube cells in FA	25
Fuel rod pitch in FA	1.26 cm
FA pitch	21.503 cm
Assembly gap	
Distance between side of pin cell and side of FA	0.0415 cm
Distance between side of pin cell and fuel rod surface	0.155 cm
Distance between fuel assemblies, fuel rod surface to surface (moderator gap)	0.393 cm

Table A.III: Fuel Assembly Types

Assembly Type	Fuel rod enrichment (wt %)	Number of burnable absorber rods in FA	Burnable absorber weight fraction (w/o)
A0	4.55	-	-
B0	4.55	32	2.0
B1	4.55	32	6.0
B2	4.55	32	8.0

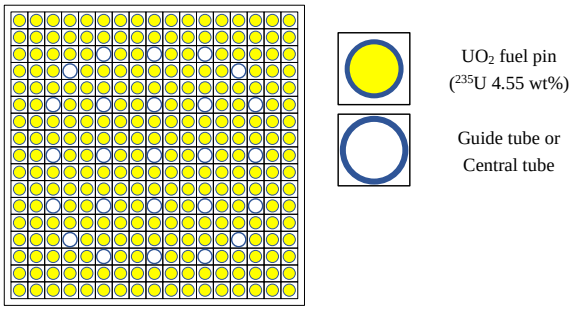

Fig. A.4. Radial Configuration of A0.

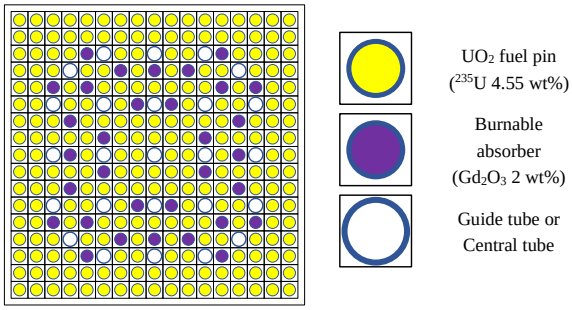

Fig. A.5. Radial Configuration of B0.

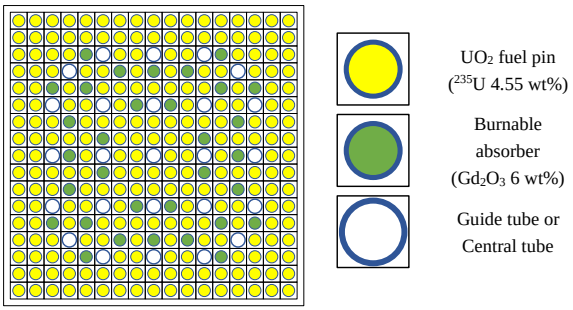

Fig. A.6. Radial Configuration of B1.

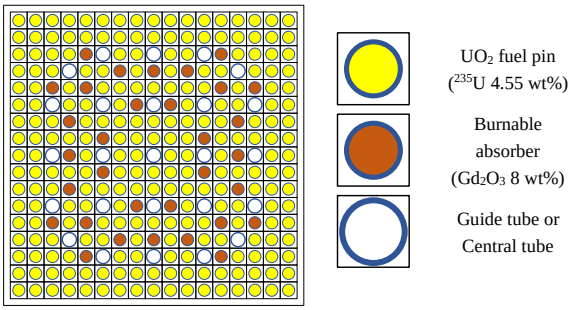

Fig. A.7. Radial Configuration of B2.

A.4 Radial Core Specification

The loading pattern of the benchmark problem is originated from the fresh core in the journal paper [2]. The loading pattern has the 45-degree symmetry. Fig.A.8 shows the radial configuration of the reactor core. The radial reflector consists of the stainless steel and the core barrel. The outside of the core barrel is filled with the moderator. Since the power distribution in the core is a major concern of this work, the problem domain is limited to the active core region and its vicinity. The dimension of radial geometry of the benchmark problem is shown in Table A.IV.

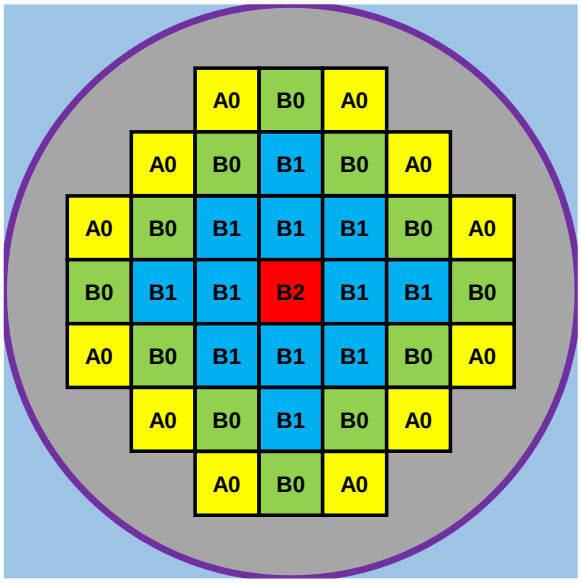

Fig. A.8. Radial Geometry of Ligh-Water SMR Core Benchmark Problem.

Table A.IV: Dimensions of Radial Geometry of Core Problems

Parameter	Value
Core	
Core lattice	7 by 7
Number of FAs	37
Assembly pitch	21.503 cm
Radial Reflector	
Radial reflector material	SS304
Distance between outer fuel rod surface and radial reflector	0.1965 cm
Core Barrel	
Core barrel material	SS304
Core barrel inner radius	93.98 cm
Core barrel outer radius	99.06 cm
Problem Domain	
Material outside the core barrel	MOD
Radial shape of the problem domain	Square
Side length of the problem domain	193.527 cm (9×21.503 cm)

A.5 Axial Geometry

This subsection describes the axial geometry for 3-D benchmark problems. Fig.A.9 shows the axial configuration of 3-D core benchmark problem. The top and bottom reflectors are homogeneous regions. They consist of moderator (MOD) and stainless steel for 20 cm height. Radial reflector and core barrel are also uniform in axial direction. The outside of the core barrel is filled with the moderator.

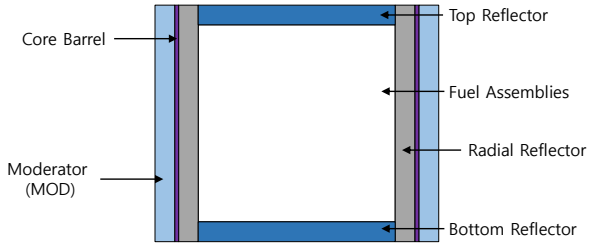

Parameter	Value
Fuel assembly height	216 cm
Top reflector height	20 cm
Bottom reflector height	20 cm
Axial reflector material	MIXREF

Fig. A.9. Axial Configuration of 3-D Core Benchmark Problem.

The geometry of fuel rod, burnable absorber rod, guide tube and central tube are shown in Fig.A.10. The height of all rods and tubes is 216 cm and the height of active fuel region is 200 cm. The fuel and burnable absorber rods have top and bottom blanket with 8.0 cm height. The top end is above the active fuel region. The axial reflectors fill the top and bottom of rods and tubes.

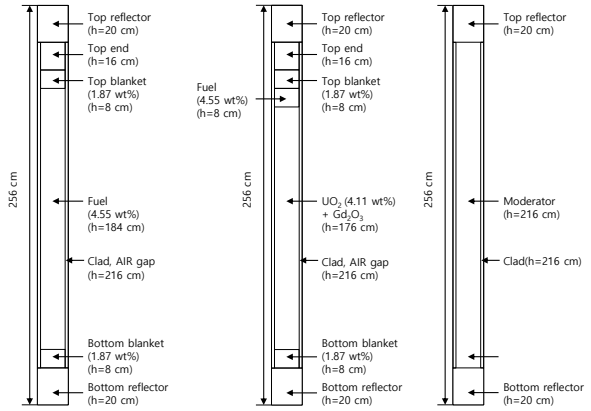

(a) Fuel rod (b) Burnable absorber rod (c) Guide/Central tube

Fig. A.10. Axial Configuration of Fuel, Burnable Absorber Rod, Guide Tube and, Central Tube.

A.6 Material Specification

Table A.V shows the list of materials defined in the previous specification. This section provides all isotope number densities for the materials in unit of [atoms/barn-cm]. The dependency of the material specification on core condition is simplified assuming that the operation parameters such as temperature and soluble boron concentration have no effects on the composition of fuel and structure. However, the materials including H2O such as the homogenized mixture materials or moderator are given depending on the operating conditions.

Table A.V: List of Materials in the Benchmark Problem

Material name	Description
UO2_187	UO_2 fuel (^{235}U 1.87 wt%) for axial blanket
UO2_455	UO_2 fuel (^{235}U 4.55 wt%)
GDw2	Gd_2O_3(2 wt%)-UO_2 (^{235}U 4.11 wt%) burnable absorber
GDw6	Gd_2O_3(6 wt%)-UO_2 (^{235}U 4.11 wt%) burnable absorber
GDw8	Gd_2O_3(8 wt%)-UO_2 (^{235}U 4.11 wt%) burnable absorber
AIR	Gap in fuel and burnable absorber
CLD	Cladding in fuel, burnable absorber rod, guide tube, and central tube
SS304	Core barrel, Radial reflector
MIXSPR	Top end of fuel, burnable absorber rods
MOD	Moderator
MIXREF	Homogenized material for axial reflector

A.6.1. Fuel, Absorber, and Structure

Table A.VI: UO_2, AIR, and Cladding Material Specification

Material name	Density [g/cm^3]	Isotope	Atomic number density [atoms/barn-cm]
UO2_187 (1.71 w/o)	10.53	^{235}U	4.44734E-04
		^{238}U	2.30430E-02
		^{16}O	4.69755E-02
		Total	7.04633E-02
UO2_455 (4.55 w/o)	10.53	^{235}U	1.08206E-03
		^{238}U	2.24128E-02
		^{16}O	4.69897E-02
		Total	7.04846E-02
AIR	0.001	^{14}N	3.29892E-05
		^{16}O	8.76928E-06
		Total	4.17585E-05
CLD	6.5	^{54}Fe	1.55685E-06
		^{56}Fe	2.44392E-05
		^{57}Fe	5.64435E-07
		^{58}Fe	7.50857E-08
		^{90}Zr	2.18488E-02
		^{91}Zr	4.76579E-03
		^{92}Zr	7.28096E-03
		^{94}Zr	7.38033E-03
		^{96}Zr	1.18858E-03
		^{93}Nb	4.21326E-04
		Total	4.29124E-02

Table A.VII: Burnable Absorber Material Specification

Material name	Density [g/cm^3]	Isotope	Atomic number density [atoms/barn-cm]
GDw2	10.422	^{235}U	9.48057E-04
		^{238}U	2.18396E-02
		^{16}O	4.66142E-02
		^{152}Gd	1.40524E-06
		^{154}Gd	1.51044E-05
		^{155}Gd	1.02500E-04
		^{156}Gd	1.41745E-04
		^{157}Gd	1.08401E-04
		^{158}Gd	1.71999E-04
		^{160}Gd	1.51421E-04
		Total	7.00945E-02

GDw6	10.228	^{235}U	8.92433E-04
		^{238}U	2.05583E-02
		^{16}O	4.59600E-02
		^{152}Gd	4.13724E-06
		^{154}Gd	4.44697E-05
		^{155}Gd	3.01776E-04
		^{156}Gd	4.17320E-04
		^{157}Gd	3.19148E-04
		^{158}Gd	5.06392E-04
		^{160}Gd	4.45808E-04
		Total	6.94497E-02
GDw8	10.133	^{235}U	8.65332E-04
		^{238}U	1.99340E-02
		^{16}O	4.56388E-02
		^{152}Gd	5.46508E-06
		^{154}Gd	5.87422E-05
		^{155}Gd	3.98630E-04
		^{156}Gd	5.51259E-04
		^{157}Gd	4.21579E-04
		^{158}Gd	6.68918E-04
		^{160}Gd	5.88890E-04
		Total	6.91316E-02

Table A.VIII: SS304 Material Specification

Material name	Density [g/cm^3]	Isotope	Atomic number density [atoms/barn-cm]
SS304	8.00	^{50}Cr	7.71070E-04
		^{52}Cr	1.48687E-02
		^{53}Cr	1.68591E-03
		^{54}Cr	4.19624E-04
		^{55}Mn	1.76615E-03
		^{54}Fe	3.54740E-03
		^{56}Fe	5.56866E-02
		^{57}Fe	1.28611E-03
		^{58}Fe	1.71088E-04
		^{58}Ni	4.74025E-03
		^{60}Ni	1.82594E-03
		^{61}Ni	7.93722E-05
		^{62}Ni	2.53073E-04
		^{64}Ni	6.44503E-05
		Total	8.71658E-02

Table A.IX: Top End Material Specification

Material name	Density [g/cm^3]	Isotope	Atomic number density [atoms/barn-cm]
MIXSPR	0.241	^{14}N	3.19995E-05
		^{16}O	8.50620E-06
		^{50}Cr	2.31321E-05
		^{52}Cr	4.46062E-04
		^{53}Cr	5.05774E-05
		^{54}Cr	1.25887E-05
		^{55}Mn	5.29844E-05
		^{54}Fe	1.06422E-04
		^{56}Fe	1.67060E-03
		^{57}Fe	3.85832E-05
		^{58}Fe	5.13265E-06
		^{58}Ni	1.42207E-04
		^{60}Ni	5.47781E-05
		^{61}Ni	2.38116E-06
		^{62}Ni	7.59219E-06
		^{64}Ni	1.93351E-06
		Total	2.65548E-03

A.6.2 Moderator and Axial Reflector

As opposed to fuel and structure, the materials in moderator and top/bottom reflector are dependent on soluble born concentrations. Table A.X shows the isotope number densities of MOD and MIXREF at 600 K depending on the soluble boron concentration. In this benchmark, it is determined that the change in the number density of other nuclides with changes in boron concentration is negligible, so the number density of other nuclides is presented as a fixed value according to boron concentration.

Table A.X: MOD and MIXREF Composition Specification

Material name	Density [g/cm^3]	Isotope	Atomic number density [atoms/barn-cm]		
			0 ppm	1000 ppm	2000 ppm
MOD (600 K)	0.66117	^{1}H	4.42147E-02	4.42147E-02	4.42147E-02
		^{10}B	0.00000E+00	7.29909E-06	1.45982E-05
		^{11}B	0.00000E+00	2.95278E-05	5.90556E-05
		^{16}O	2.21073E-02	2.21073E-02	2.21073E-02
		Total	6.63220E-02	6.63589E-02	6.63957E-02
MIXREF (600 K)	2.49588	^{1}H	3.31610E-02	3.31610E-02	3.31610E-02
		^{10}B	0.00000E+00	5.47432E-06	1.09487E-05
		^{11}B	0.00000E+00	2.21459E-05	4.42917E-05
		^{16}O	1.65805E-02	1.65805E-02	1.65805E-02
		^{50}Cr	1.92768E-04	1.92768E-04	1.92768E-04
		^{52}Cr	3.71718E-03	3.71718E-03	3.71718E-03
		^{53}Cr	4.21478E-04	4.21478E-04	4.21478E-04
		^{54}Cr	1.04906E-04	1.04906E-04	1.04906E-04
		^{55}Mn	4.41537E-04	4.41537E-04	4.41537E-04
		^{54}Fe	8.86850E-04	8.86850E-04	8.86850E-04
		^{56}Fe	1.39217E-02	1.39217E-02	1.39217E-02
		^{57}Fe	3.21527E-04	3.21527E-04	3.21527E-04
		^{58}Fe	4.27721E-05	4.27721E-05	4.27721E-05
		^{58}Ni	1.18506E-03	1.18506E-03	1.18506E-03
		^{60}Ni	4.56484E-04	4.56484E-04	4.56484E-04
		^{61}Ni	1.98430E-05	1.98430E-05	1.98430E-05
		^{62}Ni	6.32683E-05	6.32683E-05	6.32683E-05
		^{64}Ni	1.61126E-05	1.61126E-05	1.61126E-05
		Total	7.15329E-02	7.15606E-02	7.15882E-02

A.7. Calculation Conditions

Calculations will be performed at two different temperature conditions as given in Table A.XI. Table A.XII shows the reference state variables in the 3-D Core Depletion Problem. The core thermal power is 160 MWt. The moderator state is under the condition with void fraction of 0% and constant pressure of 12.76 MPa.

Table A.XI: Temperature Variations for Benchmark Problems

No.	Temperature [K]		
	Fuel	Clad	Moderator
1 (HZP)	600	600	600
2 (HFP)	900	600	600

Table A.XII: Reference State Variables for Depletion Problem

Parameter	Value
Pressure	12.76 MPa
Core Thermal Power	160 MWt
Active Core Height	200 cm

Appendix B: Definition of Benchmark Problems

B.1 Single Fuel Pin Problems

These are the single fuel pin problems. The boundary conditions are reflective radially and axially. The benchmark IDs and its calculation conditions are given in Table B.I.

Table B.I: Benchmark IDs for Single Fuel Pin Problems

No.	ID	^{235}U wt%	Temperature [K]			PPM
			Fuel	Clad	Moderator	
1	NS01C01	1.87	600	600	600	0
2	NS01C02	1.87	900	600	600	0
3	NS01C03	1.87	600	600	600	1000
4	NS01C04	1.87	900	600	600	1000
5	NS01C05	1.87	600	600	600	2000
6	NS01C06	1.87	900	600	600	2000
7	NS01C07	4.55	600	600	600	0
8	NS01C08	4.55	900	600	600	0
9	NS01C09	4.55	600	600	600	1000
10	NS01C10	4.55	900	600	600	1000
11	NS01C11	4.55	600	600	600	2000
12	NS01C12	4.55	900	600	600	2000

B.2 2-D Fuel Assembly Problems

These are the 2-D fuel assembly problems. The boundary conditions are reflective radially and axially. The benchmark IDs and its calculation conditions for each assembly are given in Table B.II.

Table B.II: Benchmark IDs for 2-D Fuel Assembly Problems

No.	ID	Type	Temperature [K]			PPM
			Fuel	Clad	Moderator	
1	NS02A0C01	A0	600	600	600	0
2	NS02A0C02	A0	900	600	600	0
3	NS02A0C03	A0	600	600	600	1000
4	NS02A0C04	A0	900	600	600	1000
5	NS02A0C05	A0	600	600	600	2000
6	NS02A0C06	A0	900	600	600	2000
7	NS02B0C01	B0	600	600	600	0
8	NS02B0C02	B0	900	600	600	0
9	NS02B0C03	B0	600	600	600	1000
10	NS02B0C04	B0	900	600	600	1000
11	NS02B0C05	B0	600	600	600	2000
12	NS02B0C06	B0	900	600	600	2000
13	NS02B1C01	B1	600	600	600	0
14	NS02B1C02	B1	900	600	600	0
15	NS02B1C03	B1	600	600	600	1000
16	NS02B1C04	B1	900	600	600	1000
17	NS02B1C05	B1	600	600	600	2000
18	NS02B1C06	B1	900	600	600	2000
19	NS02B2C01	B2	600	600	600	0
20	NS02B2C02	B2	900	600	600	0
21	NS02B2C03	B2	600	600	600	1000
22	NS02B2C04	B2	900	600	600	1000
23	NS02B2C05	B2	600	600	600	2000
24	NS02B2C06	B2	900	600	600	2000

B.3 2-D Core Problems

The problem ID and its calculation conditions for 2-D radial core are given in Table B.III. The radial boundary conditions are vacuum while it is reflective axially.

Table B.III: Benchmark IDs for 2-D Core Problems

No.	ID	Type	Temperature [K]			PPM
			Fuel	Clad	Moderator	
1	NS03C01	2-D	600	600	600	0
2	NS03C02	2-D	900	600	600	0
3	NS03C03	2-D	600	600	600	1000
4	NS03C04	2-D	900	600	600	1000
5	NS03C05	2-D	600	600	600	2000
6	NS03C06	2-D	900	600	600	2000

B.4 3-D Core Problems

The problem ID and its calculation conditions for 3-D whole core reactor are given in Table B.IV. The boundary conditions are vacuum radially and axially.

Table B.IV: Benchmark IDs for 3-D Core Problems

No.	ID	Type	Temperature [K]			PPM
			Fuel	Clad	Moderator	
1	NS04C01	3-D	600	600	600	0
2	NS04C02	3-D	900	600	600	0
3	NS04C03	3-D	600	600	600	1000
4	NS04C04	3-D	900	600	600	1000
5	NS04C05	3-D	600	600	600	2000
6	NS04C06	3-D	900	600	600	2000

B.5 3-D Core Depletion with Hot Full Power Condition

This section describes a single problem, NS05C01. NS05C01 is a 3-D whole core depletion problem in Hot Full Power (HFP) condition. Operating conditions for thermal-hydraulic feedback calculation are given in Table B.V. The problem needs critical boron concentration (CBC) search for each burnup step. The depletion calculation performs until the zero boron concentration. The xenon equilibrium state is assumed at each burnup step.

Table B.V: Problem Conditions for NS05C01

Parameter	Value
Pressure	12.76 MPa
Core Thermal Power	160 MWt
Coolant Inlet Temperature	531.45 K
Coolant Outlet Temperature	569.23 K
Coolant Mass Flow Rate	2.114×10^6 kg/hr
Control Rod State	ARO

Appendix C: Power Distribution Results of Benchmark Problems

C.1 Pin Power Distribution for 2-D Fuel Assembly Problems

X	1.0439 1.0445 0.06	1.0439 1.0443 0.04	X	1.0412 1.0422 0.09	1.0376 1.0383 0.07	X	1.0134 1.0141 0.07	0.9730 0.9705 0.26
	1.0123 1.0127 0.03	1.0123 1.0126 0.03	1.0438 1.0440 0.02	1.0107 1.0107 0.00	1.0067 1.0067 0.00	1.0304 1.0294 0.09	0.9864 0.9858 0.06	0.9678 0.9673 0.05
		1.0132 1.0127 0.05	1.0455 1.0453 0.05	1.0133 1.0142 0.09	1.0102 1.0109 0.07	1.0323 1.0324 0.01	0.9862 0.9863 0.01	0.9670 0.9665 0.05
			X	1.0520 1.0529 0.09	1.0522 1.0531 0.08	X	1.0131 1.0141 0.10	0.9699 0.9687 0.13
				1.0370 1.0391 0.20	1.0591 1.0615 0.23	1.0415 1.0435 0.19	0.9805 0.9802 0.03	0.9586 0.9582 0.04
					X	1.0200 1.0205 0.05	0.9589 0.9578 0.11	0.9477 0.9465 0.13
DeCART McCARD Err. [%]						0.9693 0.9682 0.12	0.9389 0.9383 0.07	0.9371 0.9355 0.17
							0.9284 0.9273 0.12	0.9320 0.9312 0.09
RMS Err. 0.10 % Avg. Err. 0.08 % Max. Err. 0.26 %								0.9383 0.9381 0.02

Fig. C.1. Pin Power Distribution for NS02A0C01

X	1.0440 1.0440 0.00	1.0440 1.0443 0.03	X	1.0413 1.0418 0.05	1.0376 1.0376 0.00	X	1.0134 1.0148 0.14	0.9729 0.9724 0.06
	1.0124 1.0118 0.06	1.0125 1.0124 0.01	1.0439 1.0450 0.11	1.0108 1.0110 0.02	1.0068 1.0070 0.02	1.0305 1.0306 0.01	0.9865 0.9860 0.05	0.9678 0.9673 0.06
		1.0133 1.0126 0.07	1.0456 1.0467 0.07	1.0134 1.0140 0.06	1.0103 1.0106 0.03	1.0323 1.0331 0.07	0.9862 0.9867 0.05	0.9670 0.9661 0.10
			X	1.0521 1.0523 0.01	1.0522 1.0530 0.08	X	1.0131 1.0144 0.13	0.9698 0.9683 0.15
				1.0372 1.0384 0.11	1.0594 1.0619 0.24	1.0417 1.0435 0.17	0.9805 0.9807 0.02	0.9585 0.9581 0.05
					X	1.0200 1.0209 0.08	0.9587 0.9570 0.18	0.9475 0.9460 0.16
DeCART McCARD Err. [%]						0.9692 0.9684 0.08	0.9387 0.9372 0.16	0.9369 0.9353 0.17
							0.9282 0.9262 0.22	0.9318 0.9306 0.13
RMS Err. 0.11 % Avg. Err. 0.09 % Max. Err. 0.24 %								0.9381 0.9370 0.11

Fig. C.2. Pin Power Distribution for NS02A0C02

X	1.0404 1.0409 0.05	1.0405 1.0417 0.11	X	1.0382 1.0390 0.07	1.0351 1.0345 0.06	X	1.0129 1.0129 0.00	0.9748 0.9740 0.08
	1.0103 1.0106 0.02	1.0104 1.0112 0.08	1.0405 1.0418 0.12	1.0091 1.0098 0.07	1.0056 1.0058 0.02	1.0287 1.0282 0.04	0.9871 0.9868 0.03	0.9698 0.9696 0.02
		1.0112 1.0108 0.04	1.0421 1.0422 0.04	1.0116 1.0121 0.05	1.0089 1.0090 0.00	1.0304 1.0312 0.08	0.9869 0.9870 0.01	0.9692 0.9687 0.05
			X	1.0485 1.0499 0.13	1.0490 1.0502 0.11	X	1.0128 1.0136 0.07	0.9721 0.9707 0.14
				1.0342 1.0349 0.07	1.0557 1.0578 0.20	1.0394 1.0413 0.18	0.9819 0.9816 0.03	0.9616 0.9613 0.03
					X	1.0195 1.0195 0.00	0.9618 0.9604 0.14	0.9516 0.9500 0.17
DeCART McCARD Err. [%]						0.9717 0.9704 0.13	0.9432 0.9419 0.14	0.9420 0.9402 0.19
							0.9337 0.9318 0.21	0.9374 0.9363 0.12
RMS Err. 0.10 % Avg. Err. 0.08 % Max. Err. 0.21 %								0.9437 0.9429 0.08

Fig. C.3. Pin Power Distribution for NS02A0C03

X	1.0405 1.0415 0.09	1.0406 1.0411 0.04	X	1.0383 1.0398 0.14	1.0352 1.0356 0.03	X	1.0129 1.0132 0.03	0.9747 0.9736 0.11
	1.0104 1.0110 0.06	1.0105 1.0116 0.11	1.0406 1.0406 0.00	1.0092 1.0094 0.02	1.0057 1.0067 0.10	1.0287 1.0289 0.02	0.9871 0.9872 0.01	0.9698 0.9696 0.02
		1.0114 1.0115 0.01	1.0422 1.0432 0.01	1.0117 1.0121 0.04	1.0090 1.0085 0.05	1.0305 1.0309 0.04	0.9869 0.9869 0.00	0.9691 0.9682 0.09
			X	1.0486 1.0496 0.10	1.0490 1.0493 0.03	X	1.0128 1.0137 0.09	0.9720 0.9710 0.10
				1.0344 1.0364 0.19	1.0559 1.0578 0.18	1.0396 1.0410 0.13	0.9819 0.9817 0.03	0.9615 0.9609 0.06
					X	1.0194 1.0194 0.00	0.9616 0.9601 0.16	0.9514 0.9503 0.12
DeCART McCARD Err. [%]						0.9716 0.9706 0.11	0.9430 0.9417 0.14	0.9418 0.9402 0.17
							0.9334 0.9313 0.22	0.9372 0.9355 0.18
RMS Err. 0.10 % Avg. Err. 0.08 % Max. Err. 0.22 %								0.9435 0.9430 0.06

Fig. C.4. Pin Power Distribution for NS02A0C04

X	1.0374 1.0383 0.08	1.0376 1.0376 0.00	X	1.0356 1.0361 0.05	1.0329 1.0328 0.01	X	1.0123 1.0131 0.08	0.9764 0.9745 0.19
	1.0086 1.0085 0.01	1.0088 1.0097 0.09	1.0377 1.0383 0.05	1.0078 1.0077 0.01	1.0046 1.0045 0.01	1.0271 1.0273 0.01	0.9877 0.9869 0.08	0.9716 0.9711 0.05
		1.0096 1.0098 0.02	1.0392 1.0404 0.02	1.0101 1.0099 0.02	1.0078 1.0080 0.02	1.0288 1.0288 0.00	0.9875 0.9875 0.00	0.9711 0.9708 0.04
			X	1.0454 1.0457 0.03	1.0461 1.0467 0.06	X	1.0124 1.0128 0.04	0.9741 0.9730 0.11
				1.0317 1.0326 0.09	1.0526 1.0543 0.16	1.0375 1.0390 0.14	0.9832 0.9831 0.01	0.9642 0.9639 0.03
					X	1.0189 1.0188 0.01	0.9643 0.9635 0.08	0.9550 0.9543 0.08
DeCART McCARD Err. [%]						0.9737 0.9730 0.07	0.9469 0.9466 0.03	0.9462 0.9456 0.06
							0.9383 0.9366 0.18	0.9421 0.9416 0.05
RMS Err. 0.07 % Avg. Err. 0.06 % Max. Err. 0.19 %								0.9484 0.9480 0.04

Fig. C.5. Pin Power Distribution for NS02A0C05

X	1.0375 1.0373 0.02	1.0377 1.0388 0.02	X	1.0357 1.0362 0.04	1.0330 1.0324 0.06	X	1.0123 1.0129 0.06	0.9763 0.9759 0.04
	1.0088 1.0092 0.04	1.0089 1.0096 0.07	1.0377 1.0385 0.08	1.0079 1.0082 0.02	1.0047 1.0050 0.03	1.0271 1.0268 0.03	0.9877 0.9877 0.01	0.9716 0.9722 0.06
		1.0097 1.0101 0.04	1.0393 1.0402 0.04	1.0102 1.0103 0.01	1.0079 1.0084 0.05	1.0288 1.0293 0.05	0.9876 0.9880 0.04	0.9710 0.9709 0.01
			X	1.0454 1.0461 0.06	1.0462 1.0464 0.02	X	1.0124 1.0131 0.07	0.9739 0.9728 0.11
				1.0319 1.0337 0.17	1.0528 1.0543 0.14	1.0376 1.0389 0.12	0.9832 0.9826 0.06	0.9641 0.9638 0.03
					X	1.0189 1.0191 0.02	0.9642 0.9629 0.14	0.9549 0.9540 0.10
DeCART McCARD Err. [%]						0.9736 0.9724 0.13	0.9467 0.9453 0.15	0.9460 0.9440 0.21
							0.9381 0.9361 0.21	0.9419 0.9409 0.11
RMS Err. 0.09 % Avg. Err. 0.08 % Max. Err. 0.21 %								0.9483 0.9473 0.11

Fig. C.6. Pin Power Distribution for NS02A0C06

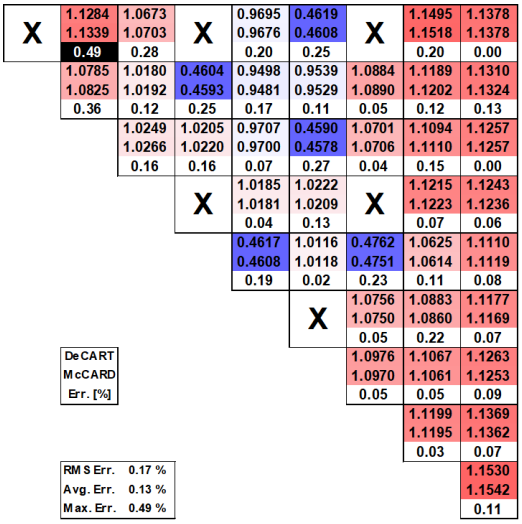

Fig. C.7. Pin Power Distribution for NS02B0C01

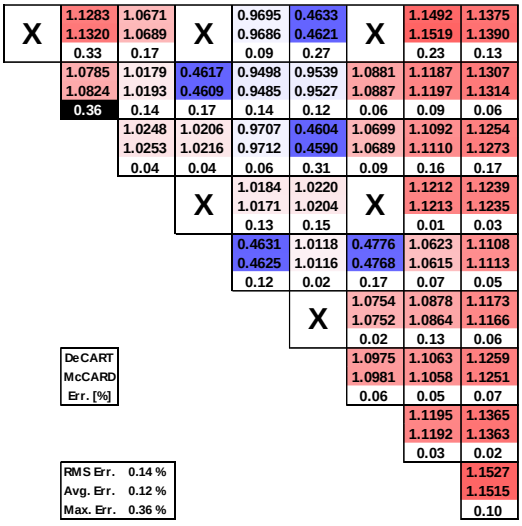

Fig. C.8. Pin Power Distribution for NS02B0C02

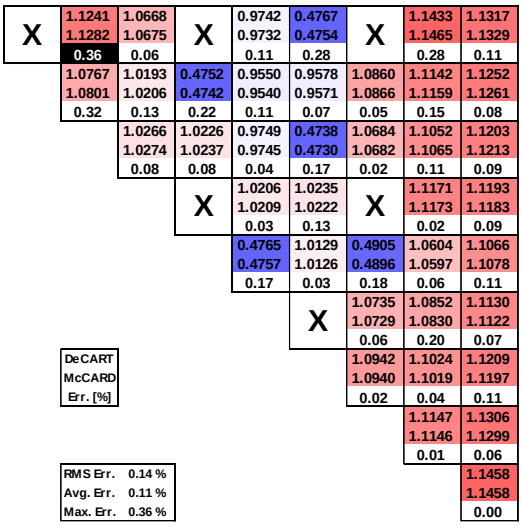

Fig. C.9. Pin Power Distribution for NS02B0C03

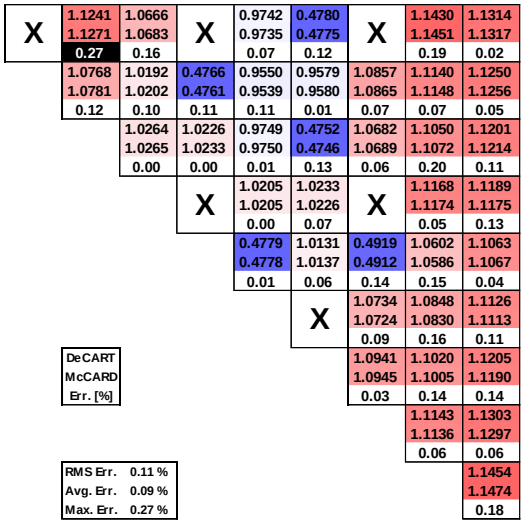

Fig. C.10. Pin Power Distribution for NS02B0C04

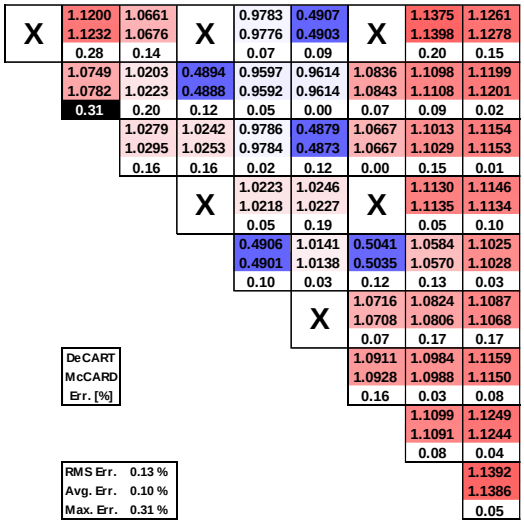

Fig. C.11. Pin Power Distribution for NS02B0C05

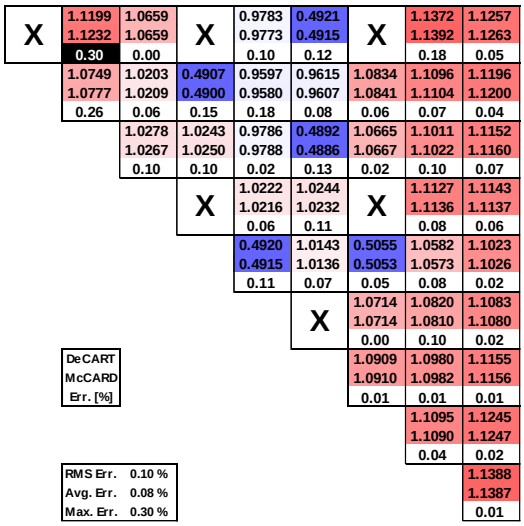

Fig. C.12. Pin Power Distribution for NS02B0C06

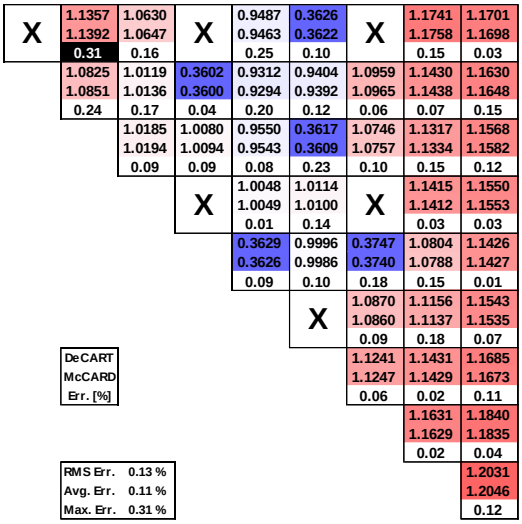

X	1.1357 1.1392 0.31	1.0630 1.0647 0.16	X	0.9487 0.9463 0.25	0.3626 0.3622 0.10	X	1.1741 1.1758 0.15	1.1701 1.1698 0.03
	1.0825 1.0851 0.24	1.0119 1.0136 0.17	0.3602 0.3600 0.04	0.9312 0.9294 0.20	0.9404 0.9392 0.12	1.0959 1.0965 0.06	1.1430 1.1438 0.07	1.1630 1.1648 0.15
		1.0185 1.0194 0.09	1.0080 1.0094 0.09	0.9550 0.9543 0.08	0.3617 0.3609 0.23	1.0746 1.0757 0.10	1.1317 1.1334 0.15	1.1568 1.1582 0.12
			X	1.0048 1.0049 0.01	1.0114 1.0100 0.14	X	1.1415 1.1412 0.03	1.1550 1.1553 0.03
				0.3629 0.3626 0.09	0.9996 0.9986 0.10	0.3747 0.3740 0.18	1.0804 1.0788 0.15	1.1426 1.1427 0.01
					X	1.0870 1.0860 0.09	1.1156 1.1137 0.18	1.1543 1.1535 0.07
	DeCART McCARD Err. [%]					1.1241 1.1247 0.06	1.1431 1.1429 0.02	1.1685 1.1673 0.11
							1.1631 1.1629 0.02	1.1840 1.1835 0.04
	RMS Err. 0.13 % Avg. Err. 0.11 % Max. Err. 0.31 %							1.2031 1.2046 0.12

Fig. C.13. Pin Power Distribution for NS02B1C01

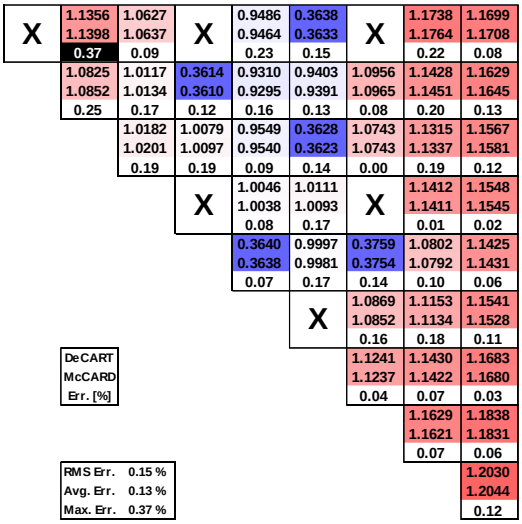

X	1.1356 1.1398 0.37	1.0627 1.0637 0.09	X	0.9486 0.9464 0.23	0.3638 0.3633 0.15	X	1.1738 1.1764 0.22	1.1699 1.1708 0.08
	1.0825 1.0852 0.25	1.0117 1.0134 0.17	0.3614 0.3610 0.12	0.9310 0.9295 0.16	0.9403 0.9391 0.13	1.0956 1.0965 0.08	1.1428 1.1451 0.20	1.1629 1.1645 0.13
		1.0182 1.0201 0.19	1.0079 1.0097 0.19	0.9549 0.9540 0.09	0.3628 0.3623 0.14	1.0743 1.0743 0.00	1.1315 1.1337 0.19	1.1567 1.1581 0.12
			X	1.0046 1.0038 0.08	1.0111 1.0093 0.17	X	1.1412 1.1411 0.01	1.1548 1.1545 0.02
				0.3640 0.3638 0.07	0.9997 0.9981 0.17	0.3759 0.3754 0.14	1.0802 1.0792 0.10	1.1425 1.1431 0.06
					X	1.0869 1.0852 0.16	1.1153 1.1134 0.18	1.1541 1.1528 0.11
	DeCART McCARD Err. [%]					1.1241 1.1237 0.04	1.1430 1.1422 0.07	1.1683 1.1680 0.03
							1.1629 1.1621 0.07	1.1838 1.1831 0.06
	RMS Err. 0.15 % Avg. Err. 0.13 % Max. Err. 0.37 %							1.2030 1.2044 0.12

Fig. C.14. Pin Power Distribution for NS02B1C02

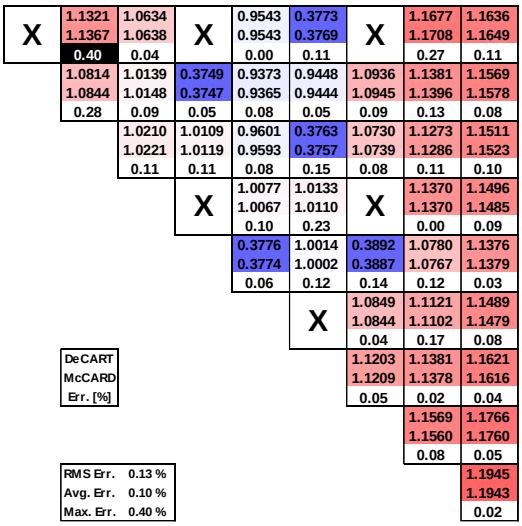

X	1.1321 1.1367 0.40	1.0634 1.0638 0.04	X	0.9543 0.9543 0.00	0.3773 0.3769 0.11	X	1.1677 1.1708 0.27	1.1636 1.1649 0.11
	1.0814 1.0844 0.28	1.0139 1.0148 0.09	0.3749 0.3747 0.05	0.9373 0.9365 0.08	0.9448 0.9444 0.05	1.0936 1.0945 0.09	1.1381 1.1396 0.13	1.1569 1.1578 0.08
		1.0210 1.0221 0.11	1.0109 1.0119 0.11	0.9601 0.9593 0.08	0.3763 0.3757 0.15	1.0730 1.0739 0.08	1.1273 1.1286 0.11	1.1511 1.1523 0.10
			X	1.0077 1.0067 0.10	1.0133 1.0110 0.23	X	1.1370 1.1370 0.00	1.1496 1.1485 0.09
				0.3776 0.3774 0.06	1.0014 1.0002 0.12	0.3892 0.3887 0.14	1.0780 1.0767 0.12	1.1376 1.1379 0.03
					X	1.0849 1.0844 0.04	1.1121 1.1102 0.17	1.1489 1.1479 0.08
	DeCART McCARD Err. [%]					1.1203 1.1209 0.05	1.1381 1.1378 0.02	1.1621 1.1616 0.04
							1.1569 1.1560 0.08	1.1766 1.1760 0.05
	RMS Err. 0.13 % Avg. Err. 0.10 % Max. Err. 0.40 %							1.1945 1.1943 0.02

Fig. C.15. Pin Power Distribution for NS02B1C03

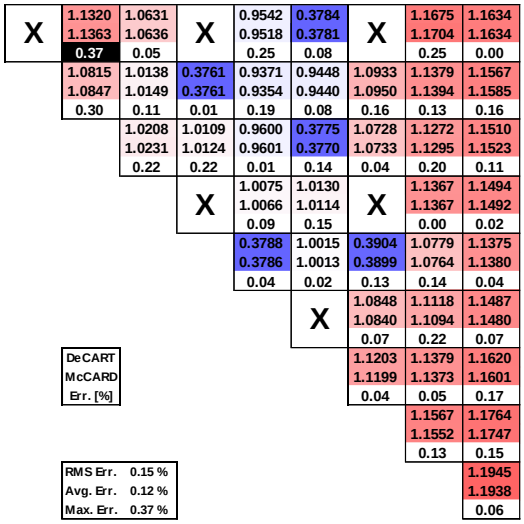

X	1.1320 1.1363 0.37	1.0631 1.0636 0.05	X	0.9542 0.9518 0.25	0.3784 0.3781 0.08	X	1.1675 1.1704 0.25	1.1634 1.1634 0.00
	1.0815 1.0847 0.30	1.0138 1.0149 0.11	0.3761 0.3761 0.01	0.9371 0.9354 0.19	0.9448 0.9440 0.08	1.0933 1.0950 0.16	1.1379 1.1394 0.13	1.1567 1.1585 0.16
		1.0208 1.0231 0.22	1.0109 1.0124 0.22	0.9600 0.9601 0.01	0.3775 0.3770 0.14	1.0728 1.0733 0.04	1.1272 1.1295 0.20	1.1510 1.1523 0.11
			X	1.0075 1.0066 0.09	1.0130 1.0114 0.15	X	1.1367 1.1367 0.00	1.1494 1.1492 0.02
				0.3788 0.3786 0.04	1.0015 1.0013 0.02	0.3904 0.3899 0.13	1.0779 1.0764 0.14	1.1375 1.1380 0.04
					X	1.0848 1.0840 0.07	1.1118 1.1094 0.22	1.1487 1.1480 0.07
	DeCART McCARD Err. [%]					1.1203 1.1199 0.04	1.1379 1.1373 0.05	1.1620 1.1601 0.17
							1.1567 1.1552 0.13	1.1764 1.1747 0.15
	RMS Err. 0.15 % Avg. Err. 0.12 % Max. Err. 0.37 %							1.1945 1.1938 0.06

Fig. C.16. Pin Power Distribution for NS02B1C04

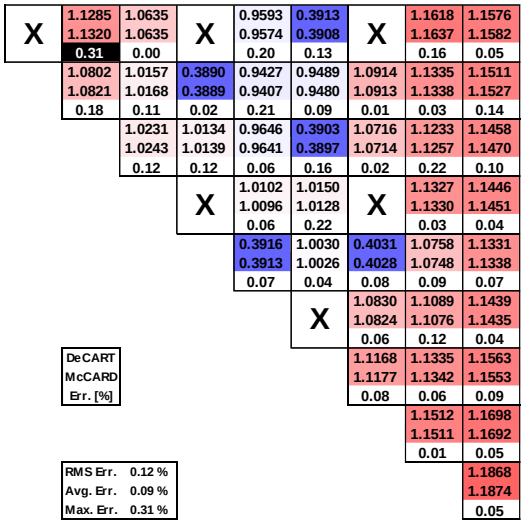

X	1.1285 1.1320 0.31	1.0635 1.0635 0.00	X	0.9593 0.9574 0.20	0.3913 0.3908 0.13	X	1.1618 1.1637 0.16	1.1576 1.1582 0.05
	1.0802 1.0821 0.18	1.0157 1.0168 0.11	0.3890 0.3889 0.02	0.9427 0.9407 0.21	0.9489 0.9480 0.09	1.0914 1.0913 0.01	1.1335 1.1338 0.03	1.1511 1.1527 0.14
		1.0231 1.0243 0.12	1.0134 1.0139 0.12	0.9646 0.9641 0.06	0.3903 0.3897 0.16	1.0716 1.0714 0.02	1.1233 1.1257 0.22	1.1458 1.1470 0.10
			X	1.0102 1.0096 0.06	1.0150 1.0128 0.22	X	1.1327 1.1330 0.03	1.1446 1.1451 0.04
				0.3916 0.3913 0.07	1.0030 1.0026 0.04	0.4031 0.4028 0.08	1.0758 1.0748 0.09	1.1331 1.1338 0.07
					X	1.0830 1.0824 0.06	1.1089 1.1076 0.12	1.1439 1.1435 0.04
	DeCART McCARD Err. [%]					1.1168 1.1177 0.08	1.1335 1.1342 0.06	1.1563 1.1553 0.09
							1.1512 1.1511 0.01	1.1698 1.1692 0.05
	RMS Err. 0.12 % Avg. Err. 0.09 % Max. Err. 0.31 %							1.1868 1.1874 0.05

Fig. C.17. Pin Power Distribution for NS02B1C05

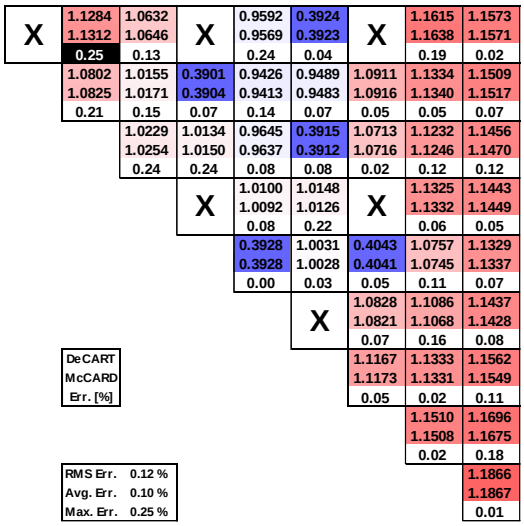

X	1.1284 1.1312 0.25	1.0632 1.0646 0.13	X	0.9592 0.9569 0.24	0.3924 0.3923 0.04	X	1.1615 1.1638 0.19	1.1573 1.1571 0.02
	1.0802 1.0825 0.21	1.0155 1.0171 0.15	0.3901 0.3904 0.07	0.9426 0.9413 0.14	0.9489 0.9483 0.07	1.0911 1.0916 0.05	1.1334 1.1340 0.05	1.1509 1.1517 0.07
		1.0229 1.0254 0.24	1.0134 1.0150 0.24	0.9645 0.9637 0.08	0.3915 0.3912 0.08	1.0713 1.0716 0.02	1.1232 1.1246 0.12	1.1456 1.1470 0.12
			X	1.0100 1.0092 0.08	1.0148 1.0126 0.22	X	1.1325 1.1332 0.06	1.1443 1.1449 0.05
				0.3928 0.3928 0.00	1.0031 1.0028 0.03	0.4043 0.4041 0.05	1.0757 1.0745 0.11	1.1329 1.1337 0.07
					X	1.0828 1.0821 0.07	1.1086 1.1068 0.16	1.1437 1.1428 0.08
	DeCART McCARD Err. [%]					1.1167 1.1173 0.05	1.1333 1.1331 0.02	1.1562 1.1549 0.11
							1.1510 1.1508 0.02	1.1696 1.1675 0.18
	RMS Err. 0.12 % Avg. Err. 0.10 % Max. Err. 0.25 %							1.1866 1.1867 0.01

Fig. C.18. Pin Power Distribution for NS02B1C06

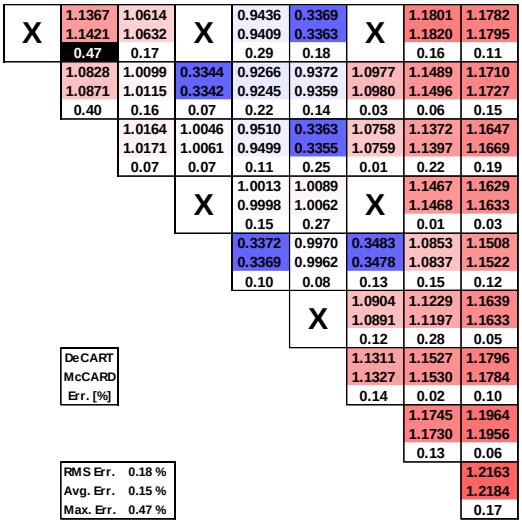

X	1.1367 1.1421 0.47	1.0614 1.0632 0.17	X	0.9436 0.9409 0.29	0.3369 0.3363 0.18	X	1.1801 1.1820 0.16	1.1782 1.1795 0.11
	1.0828 1.0871 0.40	1.0099 1.0115 0.16	0.3344 0.3342 0.07	0.9266 0.9245 0.22	0.9372 0.9359 0.14	1.0977 1.0980 0.03	1.1489 1.1496 0.06	1.1710 1.1727 0.15
		1.0164 1.0171 0.07	1.0046 1.0061 0.07	0.9510 0.9499 0.11	0.3363 0.3355 0.25	1.0758 1.0759 0.01	1.1372 1.1397 0.22	1.1647 1.1669 0.19
			X	1.0013 0.9998 0.15	1.0089 1.0062 0.27	X	1.1467 1.1468 0.01	1.1629 1.1633 0.03
				0.3372 0.3369 0.10	0.9970 0.9962 0.08	0.3483 0.3478 0.13	1.0853 1.0837 0.15	1.1508 1.1522 0.12
					X	1.0904 1.0891 0.12	1.1229 1.1197 0.28	1.1639 1.1633 0.05
	DeCART McCARD Err. [%]					1.1311 1.1327 0.14	1.1527 1.1530 0.02	1.1796 1.1784 0.10
							1.1745 1.1730 0.13	1.1964 1.1956 0.06
	RMS Err. 0.18 % Avg. Err. 0.15 % Max. Err. 0.47 %							1.2163 1.2184 0.17

Fig. C.19. Pin Power Distribution for NS02B2C01

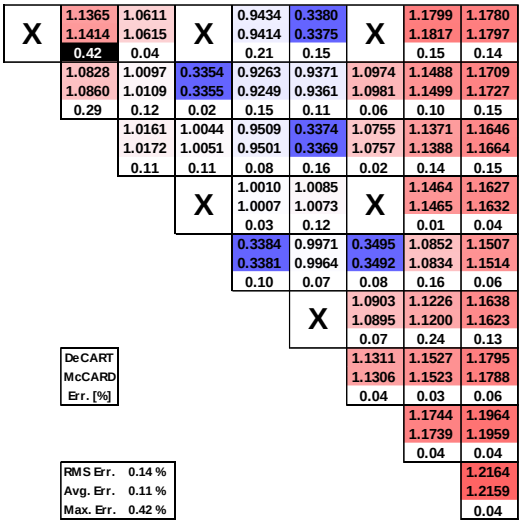

X	1.1365 1.1414 0.42	1.0611 1.0615 0.04	X	0.9434 0.9414 0.21	0.3380 0.3375 0.15	X	1.1799 1.1817 0.15	1.1780 1.1797 0.14
	1.0828 1.0860 0.29	1.0097 1.0109 0.12	0.3354 0.3355 0.02	0.9263 0.9249 0.15	0.9371 0.9361 0.11	1.0974 1.0981 0.06	1.1488 1.1499 0.10	1.1709 1.1727 0.15
		1.0161 1.0172 0.11	1.0044 1.0051 0.11	0.9509 0.9501 0.08	0.3374 0.3369 0.16	1.0755 1.0757 0.02	1.1371 1.1388 0.14	1.1646 1.1664 0.15
			X	1.0010 1.0007 0.03	1.0085 1.0073 0.12	X	1.1464 1.1465 0.01	1.1627 1.1632 0.04
				0.3384 0.3381 0.10	0.9971 0.9964 0.07	0.3495 0.3492 0.08	1.0852 1.0834 0.16	1.1507 1.1514 0.06
					X	1.0903 1.0895 0.07	1.1226 1.1200 0.24	1.1638 1.1623 0.13
	DeCART McCARD Err. [%]					1.1311 1.1306 0.04	1.1527 1.1523 0.03	1.1795 1.1788 0.06
							1.1744 1.1739 0.04	1.1964 1.1959 0.04
	RMS Err. 0.14 % Avg. Err. 0.11 % Max. Err. 0.42 %							1.2164 1.2159 0.04

Fig. C.20. Pin Power Distribution for NS02B2C02

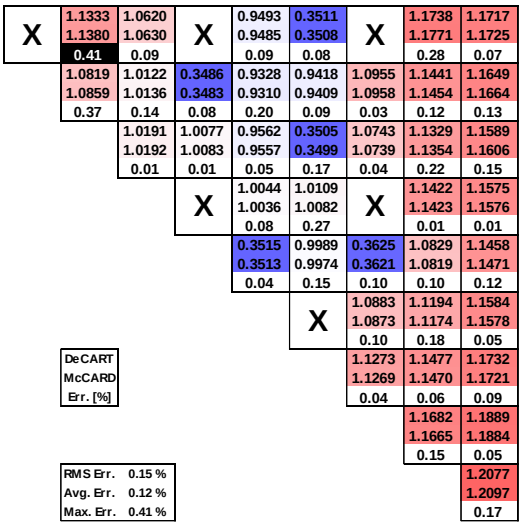

X	1.1333 1.1380 0.41	1.0620 1.0630 0.09	X	0.9493 0.9485 0.09	0.3511 0.3508 0.08	X	1.1738 1.1771 0.28	1.1717 1.1725 0.07
	1.0819 1.0859 0.37	1.0122 1.0136 0.14	0.3486 0.3483 0.08	0.9328 0.9310 0.20	0.9418 0.9409 0.09	1.0955 1.0958 0.03	1.1441 1.1454 0.12	1.1649 1.1664 0.13
		1.0191 1.0192 0.01	1.0077 1.0083 0.01	0.9562 0.9557 0.05	0.3505 0.3499 0.17	1.0743 1.0739 0.04	1.1329 1.1354 0.22	1.1589 1.1606 0.15
			X	1.0044 1.0036 0.08	1.0109 1.0082 0.27	X	1.1422 1.1423 0.01	1.1575 1.1576 0.01
				0.3515 0.3513 0.04	0.9989 0.9974 0.15	0.3625 0.3621 0.10	1.0829 1.0819 0.10	1.1458 1.1471 0.12
					X	1.0883 1.0873 0.10	1.1194 1.1174 0.18	1.1584 1.1578 0.05
	DeCART McCARD Err. [%]					1.1273 1.1269 0.04	1.1477 1.1470 0.06	1.1732 1.1721 0.09
							1.1682 1.1665 0.15	1.1889 1.1884 0.05
	RMS Err. 0.15 % Avg. Err. 0.12 % Max. Err. 0.41 %							1.2077 1.2097 0.17

Fig. C.21. Pin Power Distribution for NS02B2C03

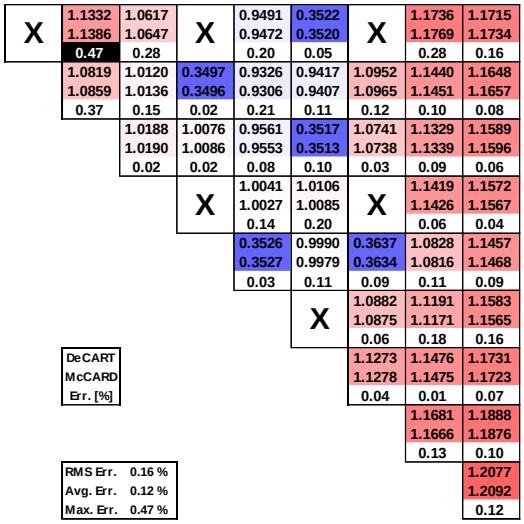

X	1.1332 1.1386 0.47	1.0617 1.0647 0.28	X	0.9491 0.9472 0.20	0.3522 0.3520 0.05	X	1.1736 1.1769 0.28	1.1715 1.1734 0.16
	1.0819 1.0859 0.37	1.0120 1.0136 0.15	0.3497 0.3496 0.02	0.9326 0.9306 0.21	0.9417 0.9407 0.11	1.0952 1.0965 0.12	1.1440 1.1451 0.10	1.1648 1.1657 0.08
		1.0188 1.0190 0.02	1.0076 1.0086 0.02	0.9561 0.9553 0.08	0.3517 0.3513 0.10	1.0741 1.0738 0.03	1.1329 1.1339 0.09	1.1589 1.1596 0.06
			X	1.0041 1.0027 0.14	1.0106 1.0085 0.20	X	1.1419 1.1426 0.06	1.1572 1.1567 0.04
				0.3526 0.3527 0.03	0.9990 0.9979 0.11	0.3637 0.3634 0.09	1.0828 1.0816 0.11	1.1457 1.1468 0.09
					X	1.0882 1.0875 0.06	1.1191 1.1171 0.18	1.1583 1.1565 0.16
	DeCART McCARD Err. [%]					1.1273 1.1278 0.04	1.1476 1.1475 0.01	1.1731 1.1723 0.07
							1.1681 1.1666 0.13	1.1888 1.1876 0.10
	RMS Err. 0.16 % Avg. Err. 0.12 % Max. Err. 0.47 %							1.2077 1.2092 0.12

Fig. C.22. Pin Power Distribution for NS02B2C04

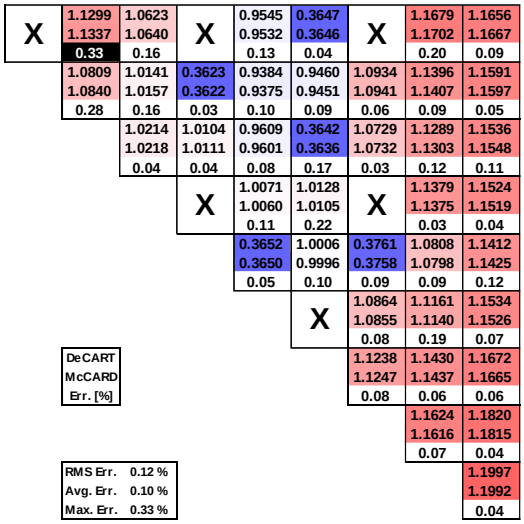

X	1.1299 1.1337 0.33	1.0623 1.0640 0.16	X	0.9545 0.9532 0.13	0.3647 0.3646 0.04	X	1.1679 1.1702 0.20	1.1656 1.1667 0.09
	1.0809 1.0840 0.28	1.0141 1.0157 0.16	0.3623 0.3622 0.03	0.9384 0.9375 0.10	0.9460 0.9451 0.09	1.0934 1.0941 0.06	1.1396 1.1407 0.09	1.1591 1.1597 0.05
		1.0214 1.0218 0.04	1.0104 1.0111 0.04	0.9609 0.9601 0.08	0.3642 0.3636 0.17	1.0729 1.0732 0.03	1.1289 1.1303 0.12	1.1536 1.1548 0.11
			X	1.0071 1.0060 0.11	1.0128 1.0105 0.22	X	1.1379 1.1375 0.03	1.1524 1.1519 0.04
				0.3652 0.3650 0.05	1.0006 0.9996 0.10	0.3761 0.3758 0.09	1.0808 1.0798 0.09	1.1412 1.1425 0.12
					X	1.0864 1.0855 0.08	1.1161 1.1140 0.19	1.1534 1.1526 0.07
	DeCART McCARD Err. [%]					1.1238 1.1247 0.08	1.1430 1.1437 0.06	1.1672 1.1665 0.06
							1.1624 1.1616 0.07	1.1820 1.1815 0.04
	RMS Err. 0.12 % Avg. Err. 0.10 % Max. Err. 0.33 %							1.1997 1.1992 0.04

Fig. C.23. Pin Power Distribution for NS02B2C05

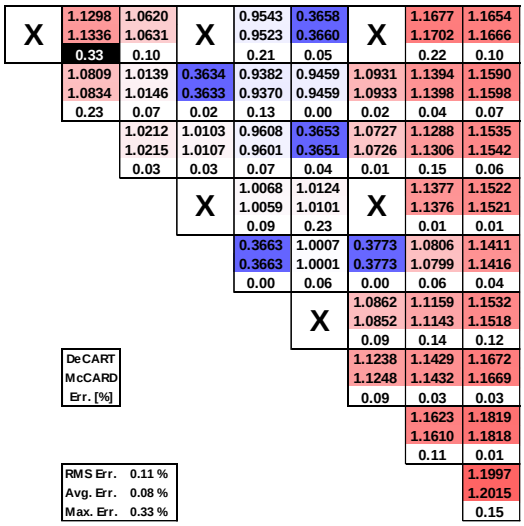

X	1.1298 1.1336 0.33	1.0620 1.0631 0.10	X	0.9543 0.9523 0.21	0.3658 0.3660 0.05	X	1.1677 1.1702 0.22	1.1654 1.1666 0.10
	1.0809 1.0834 0.23	1.0139 1.0146 0.07	0.3634 0.3633 0.02	0.9382 0.9370 0.13	0.9459 0.9459 0.00	1.0931 1.0933 0.02	1.1394 1.1398 0.04	1.1590 1.1598 0.07
		1.0212 1.0215 0.03	1.0103 1.0107 0.03	0.9608 0.9601 0.07	0.3653 0.3651 0.04	1.0727 1.0726 0.01	1.1288 1.1306 0.15	1.1535 1.1542 0.06
			X	1.0068 1.0059 0.09	1.0124 1.0101 0.23	X	1.1377 1.1376 0.01	1.1522 1.1521 0.01
				0.3663 0.3663 0.00	1.0007 1.0001 0.06	0.3773 0.3773 0.00	1.0806 1.0799 0.06	1.1411 1.1416 0.04
					X	1.0862 1.0852 0.09	1.1159 1.1143 0.14	1.1532 1.1518 0.12
	DeCART McCARD Err. [%]					1.1238 1.1248 0.09	1.1429 1.1432 0.03	1.1672 1.1669 0.03
							1.1623 1.1610 0.11	1.1819 1.1818 0.01
	RMS Err. 0.11 % Avg. Err. 0.08 % Max. Err. 0.33 %							1.1997 1.2015 0.15

Fig. C.24. Pin Power Distribution for NS02B2C06

C.2 Radial Assembly Power Distribution for 2-D Core Problems

0.8129	0.8677	0.9359	0.8294
0.8189	0.8719	0.9391	0.8248
0.74	0.48	0.34	0.56
	0.9323	1.0694	1.0465
	0.9367	1.0727	1.0401
	0.47	0.30	0.62
		1.2497	
		1.2473	
		0.19	

DeCART
McCARD
Diff. [%]

RMS Diff. 0.49 %
Avg. Diff. 0.46 %
Max. Diff. 0.74 %

Fig. C.25. Radial Assembly Power Distribution for NS03C01

0.8107	0.8661	0.9353	0.8299
0.8135	0.8700	0.9369	0.8246
0.34	0.45	0.18	0.64
	0.9312	1.0696	1.0474
	0.9350	1.0736	1.0413
	0.40	0.37	0.58
		1.2508	
		1.2503	
		0.04	

DeCART
McCARD
Diff. [%]

RMS Diff. 0.42 %
Avg. Diff. 0.37 %
Max. Diff. 0.64 %

Fig. C.26. Radial Assembly Power Distribution for NS03C02

0.8528	0.9019	0.9517	0.8264
0.8569	0.9063	0.9545	0.8207
0.48	0.48	0.29	0.70
	0.9583	1.0726	1.0183
	0.9627	1.0763	1.0112
	0.46	0.34	0.70
		1.2167	
		1.2166	
		0.01	

DeCART
McCARD
Diff. [%]

RMS Diff. 0.48 %
Avg. Diff. 0.43 %
Max. Diff. 0.70 %

Fig. C.27. Radial Assembly Power Distribution for NS03C03

0.8508	0.9004	0.9512	0.8269
0.8523	0.9018	0.9540	0.8227
0.18	0.15	0.29	0.51
	0.9572	1.0728	1.0192
	0.9605	1.0770	1.0138
	0.35	0.39	0.53
		1.2176	
		1.2163	
		0.11	

DeCART
McCARD
Diff. [%]

RMS Diff. 0.35 %
Avg. Diff. 0.31 %
Max. Diff. 0.53 %

Fig. C.28. Radial Assembly Power Distribution for NS03C04

0.8886	0.9323	0.9654	0.8234
0.8918	0.9355	0.9682	0.8183
0.35	0.34	0.28	0.63
	0.9812	1.0750	0.9938
	0.9849	1.0786	0.9881
	0.37	0.33	0.58
		1.1880	
		1.1871	
		0.08	

DeCART
McCARD
Diff. [%]

RMS Diff. 0.40 %
Avg. Diff. 0.37 %
Max. Diff. 0.63 %

Fig. C.29. Radial Assembly Power Distribution for NS03C05

0.8867	0.9309	0.9649	0.8239
0.8894	0.9351	0.9672	0.8187
0.30	0.45	0.23	0.64
	0.9802	1.0753	0.9945
	0.9844	1.0789	0.9886
	0.43	0.33	0.60
		1.1888	
		1.1874	
		0.12	

DeCART
McCARD
Diff. [%]

RMS Diff. 0.42 %
Avg. Diff. 0.39 %
Max. Diff. 0.64 %

Fig. C.30. Radial Assembly Power Distribution for NS03C06

C.3 Radial Assembly Power Distribution for 3-D Core Problems

0.8605	0.9077	0.9553	0.8228
0.8702	0.9152	0.9594	0.8166
1.11	0.81	0.43	0.76
	0.9633	1.0731	1.0137
	0.9701	1.0766	1.0051
	0.71	0.33	0.86
		1.2122	
		1.2079	
		0.36	

DeCART
McCARD
Diff. [%]

RMS Diff. 0.72 %
Avg. Diff. 0.67 %
Max. Diff. 1.11 %

Fig. C.31. Radial Assembly Power Distribution for NS04C01

0.8586	0.9063	0.9548	0.8232
0.8687	0.9149	0.9589	0.8161
1.16	0.94	0.42	0.87
	0.9622	1.0733	1.0145
	0.9698	1.0774	1.0046
	0.78	0.38	0.99
		1.2132	
		1.2092	
		0.33	

DeCART
McCARD
Diff. [%]

RMS Diff. 0.79 %
Avg. Diff. 0.74 %
Max. Diff. 1.16 %

Fig. C.32. Radial Assembly Power Distribution for NS04C02

0.8833	0.9277	0.9649	0.8225
0.8899	0.9354	0.9685	0.8159
0.74	0.82	0.37	0.80
	0.9786	1.0754	0.9965
	0.9856	1.0795	0.9871
	0.71	0.38	0.95
		1.1916	
		1.1889	
		0.23	

DeCART
McCARD
Diff. [%]

RMS Diff. 0.67 %
Avg. Diff. 0.63 %
Max. Diff. 0.95 %

Fig. C.33. Radial Assembly Power Distribution for NS04C03

0.8814	0.9263	0.9644	0.8230
0.8911	0.9348	0.9691	0.8175
1.08	0.91	0.48	0.67
	0.9776	1.0757	0.9972
	0.9839	1.0789	0.9885
	0.64	0.29	0.88
		1.1925	
		1.1872	
		0.45	

DeCART
McCARD
Diff. [%]

RMS Diff. 0.72 %
Avg. Diff. 0.67 %
Max. Diff. 1.08 %

Fig. C.34. Radial Assembly Power Distribution for NS04C04

0.9127	0.9527	0.9760	0.8203
0.9177	0.9586	0.9798	0.8137
0.54	0.61	0.39	0.81
	0.9973	1.0774	0.9763
	1.0038	1.0816	0.9678
	0.65	0.39	0.87
		1.1680	
		1.1659	
		0.18	

DeCART
McCARD
Diff. [%]

RMS Diff. 0.60 %
Avg. Diff. 0.56 %
Max. Diff. 0.87 %

Fig. C.35. Radial Assembly Power Distribution for NS04C05

0.9109	0.9514	0.9756	0.8208
0.9169	0.9578	0.9788	0.8140
0.66	0.66	0.32	0.84
	0.9964	1.0777	0.9770
	1.0028	1.0817	0.9686
	0.64	0.37	0.87
		1.1688	
		1.1668	
		0.17	

DeCART
McCARD
Diff. [%]

RMS Diff. 0.61 %
Avg. Diff. 0.57 %
Max. Diff. 0.87 %

Fig. C.36. Radial Assembly Power Distribution for NS04C06

C.4 Axial Power Distribution for 3-D Core Problems

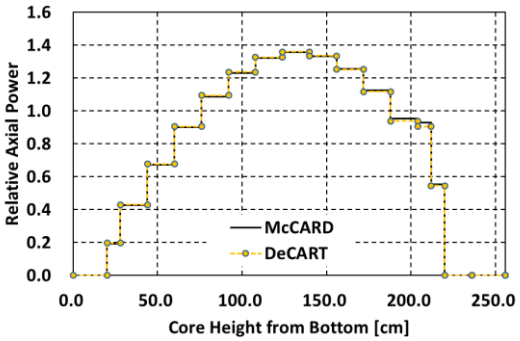

Fig. C.37. Axial Power Distribution for NS04C01

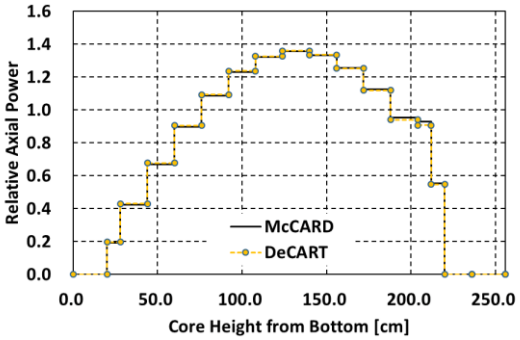

Fig. C.38. Axial Power Distribution for NS04C02

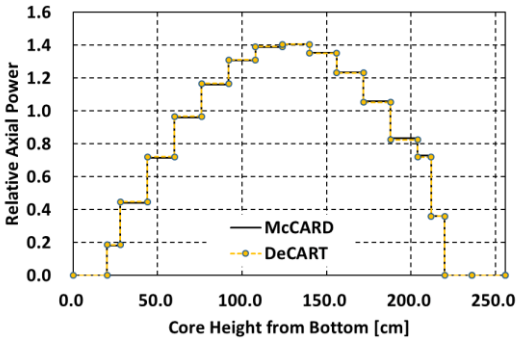

Fig. C.39. Axial Power Distribution for NS04C03

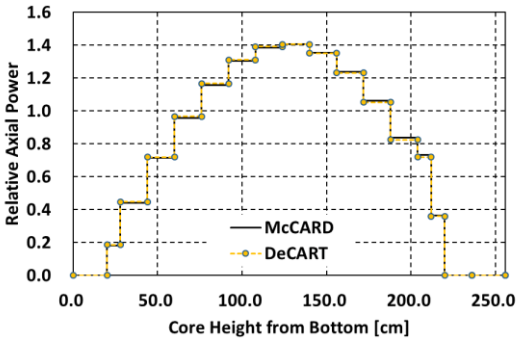

Fig. C.40. Axial Power Distribution for NS04C04

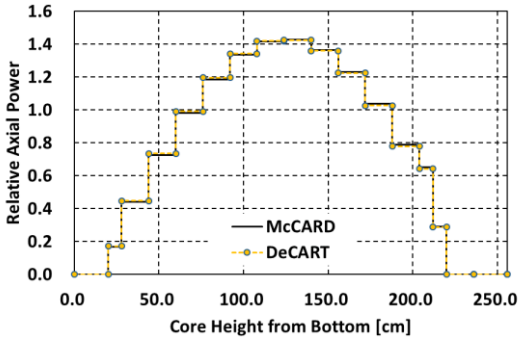

Fig. C.41. Axial Power Distribution for NS04C05

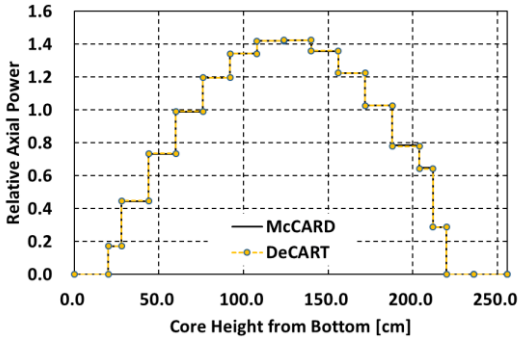

Fig. C.42. Axial Power Distribution for NS04C06